Soft Matter

Conformation changes of polyelectrolyte chains in solvent mixtures

Journal:	*Soft Matter*
Manuscript ID	SM-ART-02-2016-000352.R1
Article Type:	Paper
Date Submitted by the Author:	20-May-2016
Complete List of Authors:	Araki, Takeaki; Kyoto University, Department of Physics

ARTICLE TYPE www. rsc.org/xxxxxx | XXXXXXXX

Conformation changes of polyelectrolyte chains in solvent mixtures†

Takeaki Araki*

Received Xth XXXXXXXXXX 20XX, Accepted Xth XXXXXXXXX 20XX
First published on the web Xth XXXXXXXXXX 200X
DOI: 10.1039/b000000x

We numerically investigate behaviors of polyelectrolyte chains in solvent mixtures with taking into account the effects of the concentration inhomogeneity and the degree of the ionization. With changing the interaction parameter between the solvent components, we found a first order transition of the polymer conformation. In the mixing state far from the coexistence curve, the polymers behave as semi-flexible chains. In the phase-separated state, on the other hand, they show compact conformations included in the droplets. As the interaction parameter of the mixture is increased, the inhomogeneous concentration field develops around the polymer and it induces the critical Casimir attractive interactions among the monomers. The competition between the electrostatic interaction and the critical Casimir one gives rise to the drastic changes of the conformation.

1 Introduction

Polyelectrolytes play important roles in many systems from biology to industry. Since the conformations of polyelectrolytes affect their physical and biological properties, they have been intensively studied.[1–6] In comparison to electrically neutral polymers, polyelectrolytes are more rigid because of long-ranged electrostatic interactions among the monomers.[7,8]. They tend to behave rod-like or semi-flexible polymers in good or theta solvents. In poor solvent conditions, on the other hand, effective attractive interactions work among the monomers. These interactions lead to a variety of conformations such as sausage, toroid and necklace-like structures.[9–12]

One easily accessible way to control the interactions is to add salts. When salt is added to a polyelectrolyte solution, the electrostatic interactions among the monomers are screened and weakened. Then, the polyelectrolytes would adopt compact conformations, if the molecular attractive interactions works among the monomers. In particular, multivalent ions show drastic effects on the polyelectrolyte conformation.[13–17] They are strongly attached to the polymers, and some of them bridges the polymers, so that a smaller amount of the multivalent salt induces large conformation changes, compared to monovalent salts.

To control the interactions, solvent mixtures are also often useful.[13,14] The electrostatic interaction is inversely proportional to the dielectric constant, dependent on the mixing fraction. Then, the electrostatic interactions become stronger when a solvent of small dielectric constant is mixed. The solvent mixtures also change the electrostatic interaction in a different way. In weak polyelectrolytes, the degree of the ionization, or the electric charge, depends on the solvent.[18–23] Usually, polyelectrolytes are highly charged in water-like solutions while they are poorly charged in less polar liquids. In solvent mixtures, the ionization degree is changed with the mixing fraction.[13,24–29] It is not so simple to use solvent mixtures to control the interactions in polyelectrolytes, even if the mixtures are homogeneously mixed.

The behaviors of neutral polymers in solvent mixtures have been also studied.[30–34] The dimension of the polymer is changed when the solvent mixture approaches its critical point. There, the concentration inhomogeneity in the solvent mixture induces effective attractive interactions among the monomers. On the other hand, there are only a few studies which consider the effects of the concentration inhomogeneity on the polyelectrolytes.[27,35] To our knowledge, there is no study which considers both the contributions from the electrostatic interactions and the concentration inhomogeneity to the polymer conformation, in spite of their importance; Solvent mixtures have been importantly utilized in applications of polyelectrolytes in biology. For example, ethanol is added to aqueous solutions of polyelectrolytes, such as DNA and proteins, in order to purify and concentrate them.[14] A DNA collapses into a compact state in aqueous solutions of poly(ethylene glycol).[13,14,24,27,36] So, it is very important to understand the behaviors of polyelectrolytes in solvent mixtures.

In this article, we study the behaviors of polyelectrolytes in solvent mixtures by means of fluid particle dynamics simulation with bead-spring model.[37–39] In particular, we focus on the effects of the ionization degree and the attractive interaction, which is caused by the concentration inhomogeneity, on the conformation of the polymer chain. Here, we follow pre-

† Electronic Supplementary Information (ESI) available. See DOI: 10.1039/b000000x/

Department of Physics, Kyoto University, Sakyo-ku, Kyoto 606-8505, Japan. E-mail: araki@scphys.kyoto-u.ac.jp

vious studies on charged colloids in binary mixtures.[40] It was indicated that the inhomogeneous concentration profiles near the colloidal surfaces induce attractive interactions among the particles. The ionization degree and the affinity between the colloid and the solvent depend on the interaction parameter between the solvent components.

2 Model and simulation

2.1 Free energy

We consider polyelectrolyte chains immersed in a mixture of water-like (W) and organic (O) solvents, which are both good solvents of the polymer. The W-solvent is more polar than the other. Salt is added to the mixture and it is dissociated to monovalent ions. We describe the system with five coarse-grained variables. The polymers are described with θ (see below), and the compositions of the W- and O-solvents are $(1-\theta)\phi$ and $(1-\theta)(1-\phi)$, where $0 \leq \phi \leq 1$, respectively. The cation and anion fractions are given by c_c and c_a, respectively.

Polyelectrolyte chains are described by a particle-based model, namely, the bead-spring model. Each chain consists of N beads and the i-th bead is expressed by a shape function with a smooth profile $\theta_i(r)$ in a lattice space as[37,41]

$$\begin{aligned} \theta_i(r) &= \theta_0 h_i(r), \\ h_i(r) &= \frac{1}{2}\left\{\tanh\left(\frac{a-|r-R_i|}{d}\right)+1\right\}, \end{aligned} \tag{1}$$

where r is the lattice coordinate, a is the bead radius and d is the thickness of the bead interface. R_i is the center of the mass of the i-th bead and it is defined in an off-lattice space. In the limit of $a \gg d$, $\theta_i(r)$ approaches to θ_0 inside the bead, while it is zero in the exterior. Each bead corresponds to the Kuhn monomer[4] consisting of ν repeat units, and each repeat unit has one ionizable group. θ_0 is the density of the repeat units inside the bead and it is given by $\theta_0 = \nu v_0/V_i$, where v_0 is the volume of the repeat unit (and solvent molecules) and we assume $v_0 = d^3$. $V_i = \int dr h_i(r) (\cong 4\pi a^3/3)$ is the effective volume of the i-th bead. The distribution of the beads is defined as $\theta(r) = \sum_{i=1}^{NN_p} \theta_i(r)$, where N_p is the number of the chains in the simulation boxes.

The free energy functional consists of the following five terms,

$$\mathscr{F} = \mathscr{F}_{pol} + \mathscr{F}_{dis} + \mathscr{F}_{ion} + \mathscr{F}_{ele} + \mathscr{F}_{sol}. \tag{2}$$

The first term in the right hand side of eqn (2) is related to the bead-spring model. It is given by

$$\mathscr{F}_{pol} = \frac{K}{2}\sum_{i=1}^{N-1}(R_{i,i+1}-b)^2 + \sum_{i<j} U(R_{i,j}), \tag{3}$$

where K is the constant of the spring connecting the adjacent beads. b is the natural spring length corresponding to the Kuhn length[4] and we set $b = \nu d$. $R_{i,j} = |R_i - R_j|$ is the distance between the i-th and j-th beads. $U(R_{i,j})$ is a direct interaction between the beads. We assume short-ranged repulsive interactions of $U(R_{i,j})$ since both the solvents are good solvents. It is given by

$$U(R) = \begin{cases} U_0\{(R_{i,j}/2a)^{12} - 2(R_{i,j}/2a)^6 + 1\} & (R_{i,j} < 2a) \\ 0 & (R_{i,j} \geq 2a) \end{cases}. \tag{4}$$

$U_0 (> 0)$ is the strength of the interaction. With appropriate K, b and U_0, the polymer behaves as a self-avoiding flexible chain.

Fig. 1(a) shows a schematic picture of our bead-spring model. The circles of the solid lines indicate the beads, which correspond to the Kuhn monomers. The small circles of the broken lines represent the repeat units. In Fig. 1(a), $\nu = 4$ repeat units compose a bead. We note that the kinetics of each repeat unit is not considered in our simulations. The size of a cell grid corresponds to those of the solvent molecules and the repeat units (d) .

Since each bead contains ν ionizable groups, we treat the ionization degree with a continuous variable α, ranging from zero to unity. Depending on the local environment, it obeys the free energy of the ion dissociation given by,[23,40]

$$\begin{aligned} v_0\beta\mathscr{F}_{dis} = \int dr\theta \{&\alpha\ln\alpha + (1-\alpha)\ln(1-\alpha) \\ &+ (\Delta_0 - \Delta_1\phi)\alpha\}, \end{aligned} \tag{5}$$

where $\beta = (k_B T)^{-1}$ is the inverse of the temperature T with k_B being the Boltzmann constant. Δ_0 and Δ_1 control the dissociation. If $\Delta_1 > 0$, the ionizable groups are dissociated more in the W-solvent.

Upon the ionization, the polymer is dissociated into a negatively charged polymer and mobile cations. We assume that the counterions and the cations from the salt are the same species, so that they are described by a single variable c_c. On the other hand, the small anions originate only from the salt. The conservation of the ions and the charge neutrality condition give

$$\int dr(c_c - \alpha\theta) = \int dr c_a = c_s V_t, \tag{6}$$

where c_s is the salt concentration and V_t is the total system volume.

We assume the free energy of the ions as,[40,42–44]

$$v_0\beta\mathscr{F}_{ion} = \sum_{k=c,a}\int dr c_k \{\ln c_k - 1 - g_k(1-\theta)\phi\}, \tag{7}$$

ignoring the direct interactions between the polymer and the ions, and the volume effect of the ions.[45] g_k represents the

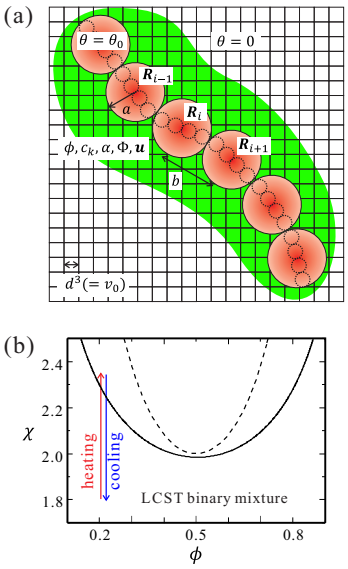

Fig. 1 (a) A schematic picture of our bead-spring model. The circles of the solid lines and the broken one indicate the beads corresponding to the Kuhn monomers and, the repeat units, respectively. a and b stand for the bead radius and the Kuhn length. The center of the mass of the i-th bead is given by R_i and it is defined in the off-lattice space. On the other hand, the solvent composition ϕ, the ion concentration c_k, the electrostatic potential Φ and the hydrodynamic flow u are calculated in the lattice space. (b) The phase diagram of the binary mixture under consideration. ϕ is the solvent composition and χ is the interaction parameter. The critical point is at $\phi = 0.5$ and $\chi = 2.0$. The solid and broken lines represent the coexistence and spinodal curves, respectively. In the simulations, we fix the averaged composition to $\bar{\phi} = 0.2$, and two paths of χ (cooling and heating) are considered (see below). With the employed parameters ($c_s \leq 4 \times 10^{-5}$ and $g_k = 2.0$), the influence of the salts on the phase diagram is negligibly small.

interaction parameters between the W-solvent and the ions ($k = \mathrm{c}, \mathrm{a}$). The affinity of the ion to a solvent is often discussed with its solvation energy in the Born model.[43] Most ions prefer to be dissolved in the water than organic solvents because the dielectric constant of the water is usually larger than those of organic solvents. The Born model is sometimes not capable of explaining some properties of the actual ion affinity.[42,46,47] For example, the correlation of the fluctuating ion concentration modifies the solvation energy and makes it dependent on the ion concentration.[47] When the water fraction is sufficiently small, the formation of a solvation shell of the water molecules gives rise to a non-linear dependence of the solvation energy on the water composition.[42] Furthermore, it is known that some organic ions show hydrophobicity.[42,43] Although the solvation energy of ions itself is difficult to model, we employ constant solvation energies g_k in this model, for simplicity. In spite of this simplification, this model can capture some essential properties of ionic systems.[40,42–44] We need to introduce more specific interactions of ions to solvents when our model is applied to specific compounds of polyelectrolyte solutions.

$\mathscr{F}_{\mathrm{ele}}$ is the electrostatic energy given by

$$\mathscr{F}_{\mathrm{ele}} = \frac{1}{8\pi} \int dr \varepsilon |\nabla \Phi|^2, \tag{8}$$

where Φ is the electrostatic potential and ε is the permittivity. We assume ε depends linearly on ϕ and the polymer fraction as

$$\varepsilon = \bar{\varepsilon} + (\varepsilon_\phi - \bar{\varepsilon})(\phi - \bar{\phi})(1-\theta) + (\varepsilon_\theta - \bar{\varepsilon})\theta/\theta_0 \tag{9}$$

with $\bar{\varepsilon}$ being the average of the permittivity. ε_ϕ and ε_θ correspond to the dielectric constants of the W-solvent and the polymer. The electrostatic potential is obtained by solving the Poisson equation,

$$\nabla \cdot (\varepsilon \nabla \Phi) = -\frac{4\pi e}{v_0} \left(\sum_{k=\mathrm{c,a}} Z_k c_k - \alpha\theta \right), \tag{10}$$

where e is the elementary electric charge. Z_c and Z_a are the valencies of the cation and anions. It is know that the polymer conformation is drastically changed when multivalent ions are added. In this study, however, we consider only monovalent ions of $Z_\mathrm{c} = -Z_\mathrm{a} = 1$, since our coarse-grained description of the ions is insufficient to consider some effects of the multivalent ions, such as ion-bridging effect.[15] In order to consider them, the particle-based description of the ions should be considered. The right hand side of eqn (10) is the local electric charge density.[23] Its last term $-\alpha\theta$ represents the electric charge of the polyelectrolytes, which are negatively charged.

The solvent free energy is given in terms of ϕ by[48]

$$v_0 \beta \mathscr{F}_{\mathrm{sol}} = \int dr \left[(1-\theta) \left\{ f(\phi) + \frac{C}{2} |\nabla \phi|^2 \right\} - g_\mathrm{p} \phi \theta \right], \tag{11}$$

$$f(\phi) = \phi \ln \phi + (1-\phi)\ln(1-\phi) + \chi\phi(1-\phi), \tag{12}$$

where χ is the interaction between the two solvents, and g_p represents the affinity between the polymer and the W-solvent. C is a constant coefficient of the gradient energy of ϕ. The phase diagram is indicated in Fig. 1(b).

2.2 Kinetics

We treat only $\phi(r)$ and $\{R_i\}$ (or $\theta(r)$) as slow variables. In other words, the ion distributions and the ionization degree are calculated by minimizing $\mathscr{F}$ with respect to c_k and α at any time t.

We readily obtained

$$v_0 \frac{\delta \beta \mathscr{F}}{\delta c_k} = \ln c_k - g_k(1-\theta)\phi + Z_k \beta e \Phi = \lambda_k, \tag{13}$$

where λ_k is a Lagrange multiplier for eqn (6). To determine λ_k ($k = \mathrm{c,a}$), we solve eqn (6) numerically (see Appendix). With substituting the solutions of eqn (13) into eqn (10), we get the Poisson-Boltzmann equation. When the polymer chain is stretched as a rod and it is highly charged, the counterion-condensation will occur.[1,4]

For the ionization degree, we also obtained

$$\alpha = [1 + \exp\{\Delta_0 - \Delta_1\phi - \beta e\Phi + \lambda_\mathrm{c}\}]^{-1}. \tag{14}$$

We note that this ionization degree depends on not only the concentration ϕ, but also the local electrostatic potential Φ and the salt concentration c_s via λ_c.

The concentration field obeys[48]

$$\frac{\partial\phi}{\partial t} = -\nabla\cdot(\phi u) + D_\phi\nabla^2\frac{\delta(v_0\beta\mathscr{F})}{\delta\phi}. \tag{15}$$

The first term of the right hand side stands for the convection by the flow $u(r)$ and D_ϕ is the diffusion constant of the solvents. The hydrodynamic flow is obtained by solving

$$\rho\frac{\partial u}{\partial t} = -\phi\nabla\frac{\delta\mathscr{F}}{\delta\phi} + \sum_i\frac{h_i(r)}{V_i}F_i - \nabla\cdot(\overleftrightarrow{\Pi} - \overleftrightarrow{\sigma}^\mathrm{R}), \tag{16}$$

where ρ is the mass density. $\overleftrightarrow{\Pi}$ is the mechanical stress tensor and is given by $\overleftrightarrow{\Pi} = p\overleftrightarrow{I} - \eta(r)\{\nabla u + (\nabla u)^\dagger\}$, where $\eta(r)$ is the viscosity. In fluid particle dynamics, it depends on the polymer distribution as $\eta(r) = \eta_0 + \Delta\eta\sum_i h_i(r)$.[37,38] η_0 is the solvent viscosity and $\eta_0 + \Delta\eta$ is that of the polymer bead. p is the pressure, which imposes the incompressible condition $\nabla\cdot u = 0$. $\overleftrightarrow{\sigma}^\mathrm{R}$ represents the random stress noise, which satisfies the fluctuation-dissipation relation at T.[49] The first term is due to the concentration inhomogeneity and includes the effect of the interface tension.[48] The second term of eqn (16) represents the force acting on the beads. F_i is given by $F_i = -\partial\mathscr{F}/\partial R_i$.[41,50]

The kinetics of the beads are solved in the off-lattice space by means of fluid particle dynamics method. The bead is transported by the hydrodynamic flow averaged inside the bead as[37]

$$\frac{d}{dt}R_i = \frac{1}{V_i}\int dr u(r)h_i(r). \tag{17}$$

Here we note the roles of the random noises in our simulation. Our model is a hybrid one, employing the field-theoretic and particle-based descriptions. The ion distributions and the ionization degree are determined by minimizing the free energy adiabatically. Also, we do not impose the random noises to ϕ, c_k and α. Thus, our model is not beyond the mean-field description when we concern the resulting interactions among the beads. Although the correlations among the electric charges would lead to interactions in the polymers[2,51], such charge correlation effects are not considered in this work.

On the other hand, we consider the conformation of the polymer chains with the particle-based description and we introduce the random noises for the chain motions via the hydrodynamic flow in eqn (16). Then, the kinetics of the polymer conformations is given by a Langevin-type equation. As we will see below, the conformation change occurs as like a first-order transition, so that the random noises for the particle motions play important roles. Such explicit conformation changes cannot be treated in the field theoretic description of the polymer chains.[52,53]

2.3 Simulation parameters

In numerical simulations, we assume the molecular size $d(= v_0^{1/3}) = 3$ Å and the bead radius $a = 2d$. Thus, each bead contains $\nu(= 2a/d) = 4$ repeat units and the repeat unit density is set to $\theta_0(\cong \nu v_0/V_i) = 0.12$. In $\mathscr{F}_\mathrm{pol}$, we set $\beta K d^2 = 10$ and $\beta U_0 = 1$, with which we ensured $|R_{i,i+1} - b| \ll d$. The average Bjerrum length is $\ell_\mathrm{B} = e^2/(4\pi\bar{\varepsilon}k_\mathrm{B}T) = 3d$, which corresponds to $\bar{\varepsilon} \cong 62$ at $T = 300$K. The ionization parameters are set $\Delta_0 = 2$ and $\Delta_1 = 10$, which give $\alpha_0 \cong 0.999$ and $\alpha_0 \cong 0.119$ for $\phi = 1$ and $\phi = 0$, respectively. Here, α_0 is obtained from $\delta\mathscr{F}_\mathrm{dis}/\delta\alpha = 0$ as $\alpha_0 = \{1 + e^{\Delta_0 - \Delta_1\phi}\}^{-1}$. In $\mathscr{F}_\mathrm{sol}$, we use $C = d^2$. A mean field theory gives the interface tension as $\gamma = k_\mathrm{B}T|\chi - 2|^{3/2}/(2d^2)$,[48] which estimates $\gamma = 4.76$mN/m at $\chi = 2.35$. The ion interaction parameters are $g_\mathrm{c} = g_\mathrm{a} = 2$, both of which correspond to the Gibbs energy of transfer of 4.99kJ/mol. The ions prefer the W-solvent (hydrophilic). For simplicity, we also set $g_\mathrm{p} = 0$, with which the polymer backbone is neutral in the affinity to the solvent components. The permittivity parameters are set to $\varepsilon_\phi = 1.4\,\bar{\varepsilon}$ and $\varepsilon_\theta = \bar{\varepsilon}$. The viscosity parameters are $\eta_0 = 0.1\,k_\mathrm{B}T/(D_\phi d)$ and $\Delta\eta = 10\,\eta_0$. Our results presented below are essentially insensitive to our choices of the parameters in η.

In this article, we fix the spatial average of the W-solvent composition at $\bar{\phi} = 0.2$. This choice of $\bar{\phi}$ is because we expect that attractive interactions caused by the inhomogeneous concentration field is strengthened when the fraction of the W-solvent is small, as in colloidal systems.[54,55] The binodal and spinodal points for $\bar{\phi} = 0.2$ are $\chi_\mathrm{t} = 2.31$ and $\chi_\mathrm{s} = 3.125$, respectively. We add the salts, the concentrations of which are set to $c_\mathrm{s} = 1\times10^{-5}$ and 4×10^{-5}. They corresponds to the Debye parameter $\kappa a = (8\pi\ell_\mathrm{B}c_\mathrm{s}/v_0)^{1/2}a \approx 0.055$ and 0.11, respectively.

It is know that the coexistence curve of the binary mixture shifts when impurities such as salts are dissolved. The degree of the change depends on the affinity of the impurity and the concentration.[43]. For our parameters of c_s and g_k, the shift of the phase separation point is negligibly small, so that we do not consider the change of the phase separation point in this study. Assuming a lower critical solution temperature (LCST)-type mixture, we consider two quench-

ing processes; heating from a mixing state with increasing χ and cooling from a phase-separated state with decreasing as shown in Fig. 1(b).

3 Results and discussions

3.1 Polymer conformations

Fig. 2(a) and (b) show the snapshots of the polyelectrolyte chains in the solvent mixtures at $\chi = 1.8$ and 2.35, respectively. We solve $N_p = 10$ chains, each of which consists of $N = 40$ beads, in a cubic box of $V_t = (256d)^3$. The volume fraction of the polymer beads is 7.9×10^{-5}. We set the salt concentration to $c_s = 4 \times 10^{-5}$. The colors of the beads represent the degree of the ionization. The interfaces between the phase-separated domains are also drawn with the isosurfaces of $\phi = 0.5$. In the mixed state far from the coexistence curve at $\chi = 1.8$ as in Fig. 1(b), the polymers behave as flexible chains. Here sharp interfaces are not formed. At $\chi = 2.35$, on the other hand, they are compartmented in the droplets of the phase-separated domains. Here, the relative fraction of the W-solvent rich phase is 0.022 and this minority phase forms the droplets. Since the droplet size is smaller than the contour length of the polymers, the polymer chains are strongly distorted by the interface tension in the droplets.

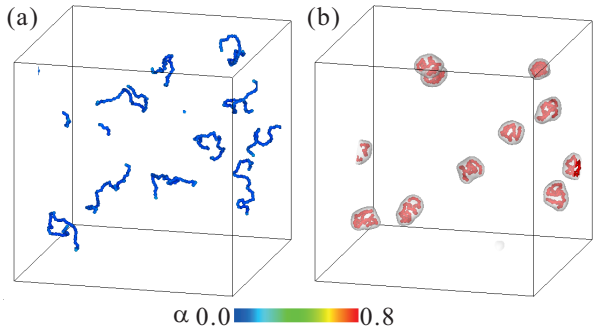

Fig. 2 The snapshots of the polymer conformations in the solvent mixtures. The interaction parameters are set to $\chi = 1.8$ in (a) and 2.35 in (b). $N_p = 10$ polymer chains, each of which consists of $N = 40$ beads, are dispersed in the cubic box with the periodic boundary conditions. The salt concentration is $c_s = 4 \times 10^{-5}$. The interfaces of the phase-separated domains are shown with the isosurfaces of $\phi = 0.5$. The colors of the beads represent the ionization.

Since the polymer volume fraction is small and the relative fraction of the W-solvent rich phase is also small, each droplet contains a single chain and the droplets are dispersed well. But, some of the polymer chains can be contained in a same droplet occasionally. In order to see detailed behaviors of the conformation changes, it is better to avoid many body effects. Then, we consider a single polyelectrolyte chain in a cuboid box, the size of which is $V_t = 256d \times (128d)^2$. The polymer is composed of $N_p = 40$ beads and its volume fraction is 3.2×10^{-4}. Since the periodic boundary conditions are employed, the simulated polymer corresponds to one of the chains in a dilute polymer solution, not an isolated one in an infinite cell.

Fig. 3(a) and (b) show their snapshots, for which χ is changed between 2.1 and 2.35. The salt concentration is $c_s = 1 \times 10^{-5}$. Assuming a lower critical solution temperature (LCST)-type mixture, we consider two quenching processes; heating from a mixed state with increasing χ in Fig. 3(a) and cooling from a phase-separated state with decreasing χ in Fig. 3(b). In Fig. 4, we plot their gyration radii R_g with respect to χ. It is calculated as

$$R_g^2 = \frac{1}{N^2} \sum_{i<j} R_{i,j}^2, \tag{18}$$

and it is averaged in a time interval $(282a^2/(6D_p) \leq t \leq 564a^2/(6D_p))$, where D_p is the diffusion constant of the particles. The simulation of a neutral polymer of $N = 40$ in the solvent of $\bar{\phi} = 0$ estimates its gyration radius as $R_g \approx 4.85\,b$. R_g of the neutral polymer is indicated by the broken line in Fig. 4. The gyration radii in the solvent mixture with $c_s = 4 \times 10^{-5}$ are also plotted.

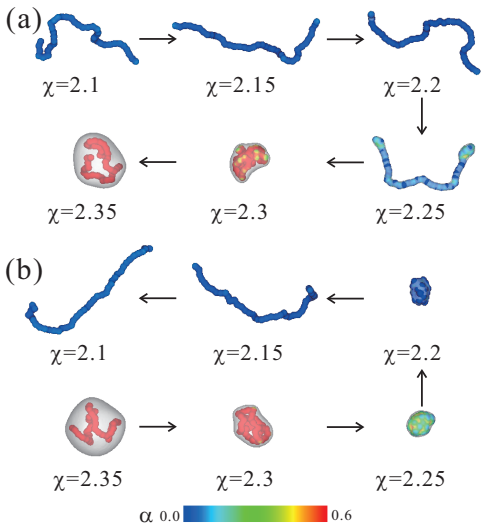

Fig. 3 The snapshots of the polymer conformation in the solvent mixture from $\chi = 2.1$ to $\chi = 2.35$. The spheres represent the beads and their colors represent the degree of the ionization. The interfaces between the phase-separated domains (grey) are also depicted with the isosurfaces of $\phi = 0.5$. Assuming a LCST mixture, the conformation changes in the (a) heating and (b) cooling processes are shown. The fraction of the W-solvent is $\bar{\phi} = 0.2$ and the salt concentration is $c_s = 1 \times 10^{-5}$, which corresponds to to $\kappa a = 0.055$.

In Fig. 3(a) and (b), we observe drastic changes of the polymer conformations. As χ is increased, an expanded chain col-

lapses into a compact state and *vice versa*. In the both cases, the polymer behaves as a flexible chain at $\chi = 2.1(< \chi_t)$. As indicated in Fig. 4, it swells larger than the neutral polymer of the same N because of the electrostatic interaction. At $\chi = 2.35(> \chi_t)$, on the other hand, the bulk mixture phase-separates and then the polyelectrolyte is covered by the minority W-rich droplet. Since the droplet radius is smaller than the gyration radius, the contributions of the electrostatic interactions and the interface tension compete in determining the droplet shape and the polymer conformation. In the cases of $\chi = 2.35$ in Figs. 3(a) and (b), the interface tension is so large that the droplet remains spherical. In the intermediate range of χ ($2.2 \le \chi \le 2.25$), the structures depend on the quenching path. This difference of the conformations is also seen in the hysteresis loop of R_g in Fig. 4, suggesting the nature of a first order transition.[27,28] It is interesting that the drastic conformation changes occur in the one-phase state of the bulk mixture ($\chi < \chi_t$).

In the cases of $c_s = 4 \times 10^{-5}$, the polymer chains tend to collapse at smaller χ, in comparison with that of $c_s = 1 \times 10^{-5}$. This is because the the salt not only weakens the electrostatic repulsions, but also enhances the affinity of the charged polymers to the W-solvent.[44] As we will see below, the affinity to one of the solvent components gives rise to the attractive interactions among the Kuhn monomers.

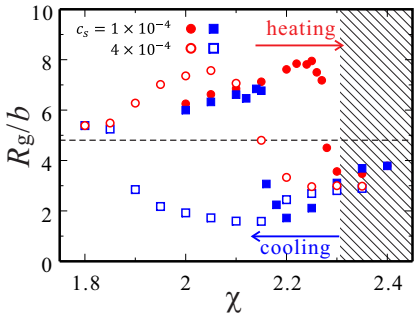

Fig. 4 The changes of the gyration radii R_g in the heating (red circle) and cooling (blue square) are plotted with respect to χ. The closed and open symbols are the gyration radii for $c_s = 1 \times 10^{-5}$ and 4×10^{-5}, respectively. The broken line is the gyration radius of a neutral polymer of the same N. The mixture of $\bar{\phi} = 0.2$ in the bulk phase-separates in the hatched region ($\chi > \chi_t$).

3.2 Ionization and adsorption

Fig. 5(a) plots the degrees of the ionization as functions of χ in the two processes of Figs. 3(a) and (b). They are averaged inside the beads as $\bar{\alpha} = \int dr \alpha(r)\theta(r) / \int dr \theta(r)$. At low χ, the ionization degrees are small and then they increase with χ. The increase of $\bar{\alpha}$ accompanies that of the electric charges. The slight increase of R_g for $\chi \le 2.25$ in the heating process (see Fig. 4) reflects the resultant enhancement of the electrostatic repulsions. We attribute the change of $\bar{\alpha}$ to that of the concentration field. The effective affinity between the polymer and the W-solvent is given by

$$\tilde{g}_p = g_p + \Delta_1 \bar{\alpha}. \tag{19}$$

Even though $g_p = 0$ as in the present simulations, the polymer tends to adsorb the W-solvent owing to $\Delta_1 \bar{\alpha}$ in $\tilde{g}_p$. In Fig. 5(b), we plot the adsorption amount Γ, which is defined as $\Gamma = \int_{\phi > \bar{\phi}} dr \phi(r)$, with χ. As χ is increased, the polymer beads adsorb more the W-solvent, since the susceptibility of the concentration field to the external field (here $\tilde{g}_p$) is increased. Since the local composition of the W-solvent is enriched around the beads, the ionizations of the beads occur more largely. Furthermore, the progress of the ionization makes the polymer more preferred to the W-solvent.[23] Thus, the ionization and the adsorption proceed with χ cooperatively. Fig. 5(b) also shows that the adsorption amount in the cooling process is larger than that in the heating one. It indicates that the compact conformations can adsorb more the W-solvent than the expanded conformations. The ionization degree in the cooling process is large compared to that in the heating process, too. This is because the larger amount of the W-solvent wets the chain in the cooling process.

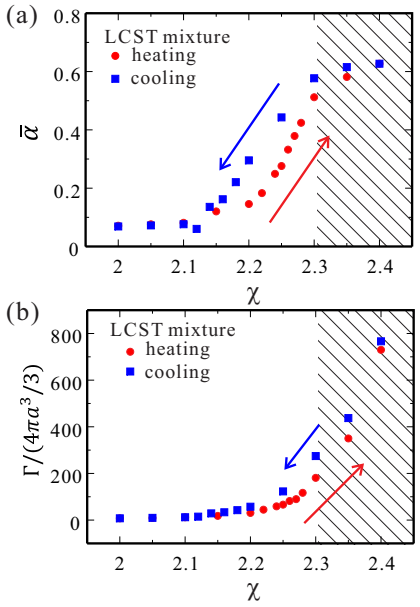

Fig. 5 Plots of the (a) the ionization degree $\bar{\alpha}$ and (b) the adsorption amount Γ as functions of χ. The fraction of the W-solvent is $\bar{\phi} = 0.2$ and the salt concentration is $c_s = 1 \times 10^{-5}$. The red circles and blue squares correspond to $\bar{\alpha}$ and Γ in the heating and cooling processes, respectively.

3.3 Pairwise interaction between two beads

The inhomogeneous concentration field induces attractive interactions among the beads. For colloidal systems, they are sometimes called as critical Casimir interaction in mixed solvents, or capillary one in phase-separated solvents. Here, we consider a bead pair ($N = 2$) to see the pairwise interaction more clearly. In Fig. 6, we plot the force $F_{1,2}$ acting on the bead pair with respect to the particle separation $R_{1,2}$. It is estimated by the spring force $F_{1,2} = K(R_{1,2} - b)$ by changing the natural spring length b. In Fig. 6, we set $\overleftrightarrow{\sigma}^{\mathrm{R}} = 0$. In the equilibrium states, this force balances with the sum of the other interactions, such that this spring force gives an estimation of the force between the non-connected beads. Its positive and negative values mean repulsive and attractive interactions, respectively. The salt concentration is set to $c_s = 1 \times 10^{-5}$. Fig. 6 shows the force consists of a short-ranged attraction and a long-ranged repulsion as reported for colloidal systems.[40] The former attraction is due to the inhomogeneous concentration field and the latter repulsion comes from the electrostatic interaction. As χ is increased, the repulsive interaction becomes strong for large $R_{1,2}$. This is because the ionization degree is increased with χ as in Fig. 5(a). Also, the range showing the attractive force expands, and the corresponding force becomes negatively large with increasing χ. The critical Casimir interaction (or the capillary interaction) work between the beads when the enriched profiles of the W-solvent around the beads overlap each other. As like in Fig. 5(b), the adsorption layer of the W-solvent develops with χ, so that the inhomogeneous concentration profiles can overlap easily when χ is large, even for large separations. The changes of the force curves lead to the conformation changes seen in Fig. 3. However, the force curves themselves cannot explain the hysteresis behaviors of R_g in Fig. 4. The combination of the total interactions among the beads and the conformation entropy would give rise to the first order transition suggested in Figs. 3 and 4.[27,28]

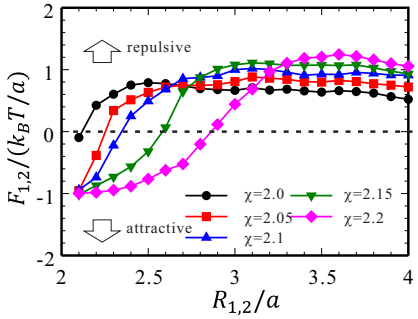

Fig. 6 The sum of the electrostatic repulsive force and the attractive force caused by the inhomogeneous concentration field for the bead pair ($N = 2$) is plotted with the particle separation $R_{1,2}$. It is estimated by the spring force $F_{1,2} = K(R_{1,2} - b)$ by changing b. The positive and negative values indicate the repulsive and attractive interactions work between the two beads, respectively. The interaction parameter is changed from $\chi = 2.0$ to 2.2.

4 Conclusions and future works

In this article, we numerically study the conformations of polyelectrolytes in solvent mixtures. We take into account the electrostatic interaction, the effective interaction induced by the concentration inhomogeneity and the ionization degree simultaneously. We observe drastic changes of the conformation and a hysteresis loop of R_g with changing the interaction parameter between the solvent components. Approaching the phase separation point, the inhomogeneous concentration field develops around the beads and it induces the attractive interactions among the beads. With these attractive interactions, the polymer collapses into a compact conformation against the electrostatic repulsions. We also found the ionization degree and the inhomogeneous concentration field develop with the interaction parameter in a cooperative way.

Our simulations demonstrate the collapsed state of polyelectrolytes in the mixed state of a solvent mixture. They may suggest an aggregation and precipitation of polyelectrolyte chains in solvent mixtures, which do not show phase separation, as observed in so-called ethanol precipitation of DNA. Addition of an organic liquid reduces the dielectric constant of the solvent and strengthens the electrostatic interactions among the ions and polymers. The stable ionic bonds between the polymers and the counterions are formed, and then the polymers become uncharged. The uncharged chains will aggregate and precipitate. Usually, the solvent mixture is considered to be well mixed, since it does not show the phase separation at any accessible temperature.

Addition of salt into a mixed solvent sometimes leads to the phase separation, that is, salting out. We consider that the phase separation might be induced locally around the polyelectrolytes and the interface tensions works to aggregate them, even if the mixture appears to be mixed macroscopically. In order to confirm this mechanism in actual polyelectrolyte solutions, some experimental observations are desired. However, it would be not easy to measure the interface tension of such droplets of a molecular scale size. If we can measure the local contents of the W-solvent and the ions in the aggregates, and they are larger than those in the supernatant, they would support our mechanism.

We have many parameters in our model. The results we presented here were limited in the choice of the parameters so that we could not discuss the behaviors in a wide range of the parameters. Other choices of the parameters such as $\bar{\phi}$, c_s and g_k would give richer and more interesting behaviors of polyelectrolytes in solvent mixtures. We will enumerate what

we should do below. We hope to report some results about them in a near future.

(i) The composition of the mixture can be controlled easily. In this study, we consider only an asymmetric mixture ($\bar{\phi} = 0.2$), with which we expect the interaction caused by the inhomogeneous concentration field is strengthened as in colloidal systems. However, other conformations will be observed, when the mixing fraction is changed. With approaching to the critical point in a symmetric mixture ($\bar{\phi} = 0.5$), the interface tension is reduced[48] and the effective attractive interaction would be also weakened. Our preliminary simulations indicate that the non-spherical domains containing semiflexible chains, which are expanded by the electrostatic repulsion, are formed (not shown here).

In the present simulations, both of the relative fraction of the W-solvent rich phase and the polymer fractions are small even in the two phase region ($\chi > \chi_t$). Then, we observe each polymer chain is compartmented in a droplet of the W-solvent rich phase in Fig. 2. If we increase them, we will see that some polyelectrolytes are confined in a same droplet. With changing the interaction parameter χ, aggregates of the polymer chains will be also observed. Aggregation process of polyelectrolytes via the mechanisms discussed above is an interesting problem.

In Figs. 2 and 3, the polymer forms a compact conformation in the phase-separated state ($\chi > \chi_t$). This is because the diameters of the droplets are shorter than the polymer contour length. Since the periodic boundary conditions are employed, the maximum droplet size is uniquely determined by the relative fraction of the phase-separated domain and the simulation box size. If we consider an isolated chain in a larger cell or an infinite one, the droplet of the minority phase will grow larger than the polymer size and the polymer will adopt more relaxed conformation in the droplet. In this sense, the gyration radius of the polyelectrolyte will depend on the system size. Also, we fix the total amount of the salt at a constant in the simulations. If we are interested in the infinite cell, we had better to control its chemical potential of the ions, not their total amounts. This difference may lead to some quantitatively different results.

(ii) The salt concentration is also an important parameter, which is easy to change. Although only the two salt concentrations are employed and the difference between them is not large, a quantitatively large difference in the conformation changes is observed (Fig. 4). If we change the salt concentration in wider range, more drastic conformation changes will be observed. In particular, it is expected that the polyelectrolyte chain will behave as a neutral polymer when a sufficiently large amount of salt is added. However, our present simulation scheme does not apply to such a high salinity limit as noted in the Appendix A. It is desired to improve the simulation method.

Also, we treat the ions by means of a coarse-grained model, namely, Poisson-Boltmann equation. Then, we do not consider the multivalent ions[15–17] and the correlation effect of the fluctuating ions.[2,51] We have to treat the ions by a particle-based model, in order to see these effects.

(iii) Although the dependence of the conformation on the chain length is quite important[4], our polymer chains consist only of $N = 40$ beads. Our simulations with shorter chains ($N = 10$ and 20) (not presented here) give an essentially same behaviors that we reported in this article. But, some qualitatively different behaviors may be observed when longer chains are used. For example, when a long charged polymer collapses into a compact conformation, the electrostatic repulsions among the monomers become enlarged. When the droplet of the finite interface tension no longer confine the polymer, Coulomb explosion locally occurs and some complex structure as a necklace may be formed.[4] In the solvent mixtures, the ions are strongly confined in the W-solvent rich domain because of the solvation energy. Then, the entropic gain of the counterions is possibly different from that in a one-component solvent. To consider it, another scaling theory should be developed.

Also from the viewpoint of the phase separation, the usage of long polymer chains will be interesting. As shown in Figs. 2 and 3, the polyelectrolytes chain behave as nuclei for the phase separation near $\chi = \chi_t$. It is know that the interface tension suppresses the formation of small droplets of the minority phase. So, when long polyelectrolytes are dissolved, they may induce the phase separation more efficiently. Although the usage of long polymers is imporant and interesting, it is not easy to simulate them. When we use longer chains, we have to carry out simulations with much longer annealing time to equilibrate the system. Simulation improvements are desired.

(vi) In this work, we do not change the material parameters, such as g_k, Δ_0 and Δ_1. In particular, the simulated solvation energy g_k is rather small, in comparison with actual ions and solvents. Not only the addition of salt of large g_k changes the phase diagram largely, but also, it will enhance the interaction between the charged polymer and the solvent.[44] Although our present simulation cannot adopt large g_k, we have to consider its influence seriously. Also, Δ_1 plays an important role in our mechanism. The dependence of the conformation on it is also needed to consider.

Acknowledgements

We acknowledge valuable discussions with A. Onuki, H. Tanaka and Y. Uematsu. This work was supported by KAKENHI (nos 25000002 and 25610122). Computation was done using the facilities of the Supercomputer Center, the Institute for Solid State Physics, the University of Tokyo. This research was also partly supported by CREST, JST.

Appendix

A Simulation scheme

Our simulation model deals with the lattice and off-lattice spaces. The solvent composition ϕ, the ion concentration c_k, the local ionization degree α, the electrostatic potential Φ and the hydrodynamic flow u are solved in the lattice space. The grid size of the lattice space is set to d as shown in Fig. 1(a), and the periodic boundary conditions are employed. Here we describe our simulation scheme.

(i) First, we determine c_k, Φ and α recursively, since they are coupled complicatedly. At this stage, we fix $\theta(t)$ and $\phi(t)$. The electrostatic potential $\Phi^{(p)}$ is obtained from eqn (10) with $c_k = c_k^{(p)}$ and $\alpha = \alpha^{(p)}$ by means of the Crank-Nikolson method. Here the suffix $p(=0,1,2,\cdots)$ indicates the iteration index. (As the initial condition for the iterations at $t=0$, we set $c_k^{(0)} = c_s$ and $\alpha^{(0)} = \{1+e^{\Delta_0-\Delta_1\bar{\phi}}\}^{-1}$. Otherwise, we set $c_k^{(0)} = c_k(t)$ and $\alpha^{(0)} = \alpha(t)$.) We calculate the Lagrange multipliers as

$$\lambda_c^{(p)} = \ln\left\{\frac{c_s V_t + \int dr \alpha^{(p)}\theta}{\int dr \exp\{g_c(1-\theta)\phi - \beta e\Phi^{(p)}\}}\right\} \quad (20)$$

$$\lambda_a^{(p)} = \ln\left\{\frac{c_s V_t}{\int dr \exp\{g_a(1-\theta)\phi + \beta e\Phi^{(p)}\}}\right\} \quad (21)$$

from eqs. (6). Then, we will have $\alpha^{(p+1)}$ and $c_k^{(p+1)}$. Solving eqn (10) with them, we obtain the electrostatic potential at the next iteration $\Phi^{(p+1)}$. We iterate the above calculations until $\lambda_k^{(p)}$ converges to a certain value, and then, we obtain $c_k(t+\Delta t)$ and $\alpha(t+\Delta t)$.

We should note that the range of the salt concentration is limited in our scheme. To solve the electrostatic potential in the lattice space, the Debye screening length should be longer that the simulation grid length d. Since the ions prefer to be dissolved in the W-solvent, their concentrations in the droplets of the W-solvent rich phase becomes much larger than their spatial averages. Then, we have to keep the salt concentration to be so small that the Debye screening length remains longer than the grid size even in the W-solvent rich phase. On the other hand, the concentration of the counterions in the simulation box is about 2×10^{-5} when the polyelectrolyte chain is highly charged, so that the solution of $c_s = 1\times10^{-5}$ corresponds to a low salinity solution.

(ii) We calculate the hydrodynamic flow u by means of Maker and cell method.[56] The flow vector field is defined in a staggered lattice. Since the Reynolds number is considered negligibly small, we iterate to develop eqn (16) without updating ϕ and θ until $\int dr|\rho\partial u/\partial t|/\int dr| - \phi\nabla\delta\mathscr{F}/\delta\phi + \sum_i h_i F_i/V_i| < 10^{-3}$. The fluid particle dynamics method was originally developed to consider colloidal suspensions in a simple liquid. In the limits of $\Delta\eta/\eta_0 \to \infty$ and $d/a \to 0$, this method is able to describe solid spherical particles with the hydrodynamic interactions with high accuracy. Since we do not need to consider the boundary conditions at the colloidal surfaces, we can calculate the hydrodynamic flow efficiently, and then, this method has been applied to some systems. The details of this numerical scheme is given elsewhere.[38] In this study, the beads do not represent colloid particles, so that we use a moderate value of $\Delta\eta/\eta_0$.

(iii) Now, we know u, c_k and α. We update the bead positions R_i and the concentration field by means of the explicit Euler scheme with the same time increment $\Delta t = 10^{-2}d^2/D_\phi$. The new polymer field θ is given by eqn (1). Then we return to (i) with using $\theta(t+\Delta t)$ and $\phi(t+\Delta t)$, instead of $\theta(t)$ and $\phi(t)$.

References

1 F. Oosawa, *Polyelectrolyte*, Mercel Dekker, New York, 1971.
2 J.-L. Barrat and J.-F. Joanny, *Adv. Chem. Phys.*, 1996, **94**, 1-66.
3 C. Holm, J.-F. Joanny, K. Kremer, R. R. Netz, P. Reineker, T. A. Seidel, C. Vilgis, and R. G. Winkler, *Adv. Polym. Sci.*, 2004, **166**, 67-111.
4 A. V. Dobrynin and M. Rubinstein, *Prog. Polym. Sci.*, 2005, **30**, 1049-1118.
5 M. Rubinstein and G. A. Papoian, *Soft Matter*, 2012, **8**, 9265-9267.
6 Y. Uematsu and T. Araki, *J. Chem. Phys.*, 2013 **139**, 094901.
7 T. Odijk, *J. Polym. Sci. part B: Polym. Phys.*, 1977, **15**, 477-483.
8 J. Skolnick and M. Fixman, *Macromolecules*, 1977, **10**, 944-948.
9 A. R. Khokhlov, *J. Phys. A: Math. Gen.*, 1980, **13**, 979-987.
10 G. E. Plum, P. G. Arscott, and V. A. Bloomfield, *Biopolym.*, 1990, **30**, 631-643.
11 A. V. Dobrynin, M. Rubinstein and S. P. Obukhov, *Macromolecules*, 1996, **29**, 2974-2979.
12 H. J. Limbach and C. Holm, *Computer Physics Communications*, 2002, **147**, 321-324.
13 V. A. Bloomfield, *Biopolym.*, 1991, **31**, 1471-1481.
14 V. A. Bloomfield, *Curr. Opin. Struct. Biol.*, 1996, **6**, 334-341.
15 E. Raspaud, M. Olvera de la Cruz, J.-L. Sikorav, and F. Livolant, *Biophys. J.*, 1998, **74**, 381-393.
16 B. I. Shklovskii, *Phys. Rev. Lett.*, 1999, **82**, 3268-3271.

17 P.-Y. Hsiao and E. Luijten, *Phys. Rev. Lett.*, 2006, **97**, 148301.

18 E. Raphael and J.-F. Joanny, *Europhys. Lett.*, 1990, **13**, 623-628.

19 I. Borukhov, D. Andelman and H. Orland, *Europhys. Lett.*, 1995, **32**, 499-504.

20 I. Borukhov, D. Andelman, R. Borrega, M. Cloitre, L. Leibler, and H. Orland, *J. Phys. Chem. B*, 2000, **104**, 11027-11034.

21 Y. Burak and R. R. Netz, *J. Phys. Chem. B*, 2004, **108**, 4840-4849.

22 R. Okamoto and A. Onuki, *J. Chem. Phys.*, 2009 **131**, 094905.

23 A. Onuki and R. Okamoto, *J. Phys. Chem. B*, 2009, **113**, 3988-3996.

24 L. S. Lerman, *Proc. Nat. Acad. Sci. USA*, 1971, **68**, 1886-1890.

25 H. L. Frisch and S. J. Fesciyan, *J. Polym. Sci. Lett. Ed.*, 1979, **17**, 309-315.

26 P. G. Arscott, C. Ma, J. R. Wenner and V. A. Bloomfield, *Biopolym.*, 1995, **36**, 345-364.

27 V. V. Vasilevskaya, A. R. Khokhlov, Y. Matsuzawa, and K. Yoshikawa, *J. Chem. Phys.*, 1995, **102**, 6595-6602.

28 M. Ueda and K. Yoshikawa, *Phys. Rev. Lett.*, 1996, **77**, 2133-2136.

29 S. M. Mel'nikov, M. O. Khan, B. Lindman and B. Jönsson, *J. Am. Chem. Soc.*, 1999, **121**, 1130-1136.

30 A. R. Shultz and P. J. Flory, *J. Polym. Sci.*, 1955, **15**, 231-242.

31 F. Brochard and P. G. de Gennes, *Ferroelectrics*, 1980, **30**, 33-47.

32 J. J. Magda, G. H. Fredrickson, R. G. Larson, and E. Helfand, *Macromolecules* 1988, **21**, 726-732.

33 K. To and H. J. Choi, *Phys. Rev. Lett.*, 1998, **80**, 536-539.

34 C. A. Grabowski and A. Mukhopadhyay, *Phys. Rev. Lett.*, 2007, **98**, 207801.

35 D. Baigl and K. Yoshikawa, *Biophys. J.*, 2005, **88**, 3486-3493.

36 D. Ben-Yaakov, D. Andelman, D. Harries and R. Podgornik, *J. Phys. Chem. B*, 2009, **113**, 6001-6011.

37 H. Tanaka and T. Araki, *Phys. Rev. Lett.*, 2000, **85**, 1338-1341.

38 H. Tanaka and T. Araki, *Chem. Eng. Sci.*, 2006, **61**, 2108-2141.

39 K. Kamata, T. Araki and H. Tanaka, *Phys. Rev. Lett.* 2009, **102**, 108303.

40 R. Okamoto and A. Onuki, *Phys. Rev. E*, 2011, **84**, 051401.

41 T. Araki and H. Tanaka, *Phys. Rev. E*, 2006, **73**, 061506.

42 A. Onuki, R. Okamoto and T. Araki, *Bull. Chem. Soc. Jpn.*, 2011, **84**, 569-587.

43 A. Onuki and R. Okamoto, *Curr. Opin. Colloid Interface Sci.*, 2011, **16**, 525-533.

44 S. Samin and Y. Tsori, *J. Chem. Phys.*, 2012, **136**, 154908.

45 D. Ben-Yaakov, D. Andelman, D. Harries and R. Podgornik, *J. Phys.: Condens. Matter*, 2009, **21**, 424106.

46 Z.-G. Wang, *J. Phys. Chem. B*, 2008, **112**, 16205.

47 Z.-G. Wang, *Phys. Rev. Lett.* 2010, **81**, 021501.

48 A. Onuki, *Phase Transition Dynamics*, Cambridge Univ. Press, Cambridge, 2002.

49 A. Furukawa and H. Tanaka, *Phys. Rev. Lett.*, 2010, **104**, 245702.

50 T. Araki and H. Tanaka, *J. Phys.: Condens. Matter*, 2008, **20**, 072101.

51 B.-Y. Ha and A. J. Liu, *Phys. Rev. Lett.*, 1997, **79**, 1289-1929.

52 Y. O. Popov, J. Lee and G. H. Fredrickson, *J. Polym. Sci., Part B: Polym. Phys.*, 2007, **45**, 3223-3230.

53 R. A. Riggleman and G. H. Fredrickson, it J. Chem. Phys., 2010, **132**, 024104.

54 D. Beysense and D. Estève, *Phys. Rev. Lett.*, 1985, **54**, 2123-2126.

55 R. Okamoto and A. Onuki, *J. Chem. Phys.*, 2012, **136**, 114704.

56 F. H. Harlow and H. E. Welch, *Phys. Fluids*, 1965, **8**, 2182-2189.

With changing the interaction parameter in a solvent mixture, semi-flexible polyelectrolyte chains transform to compact conformations discontinuously.

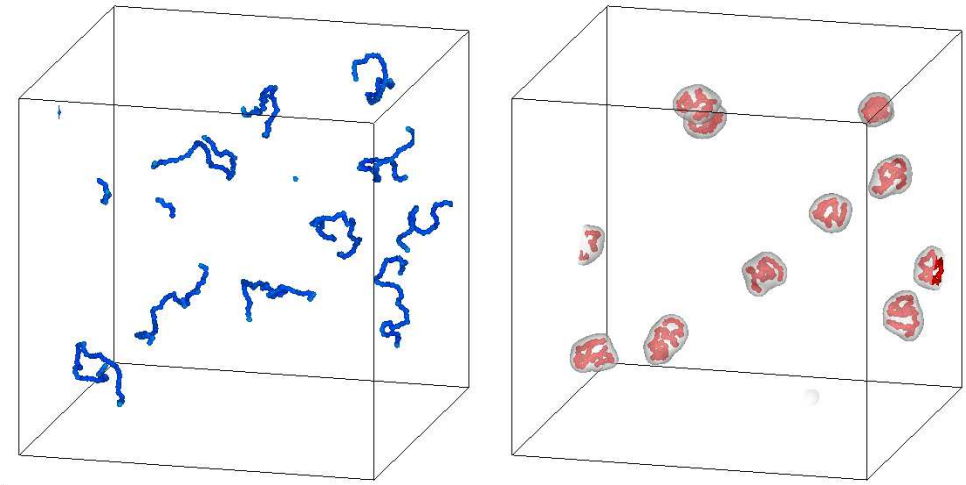

$\chi < \chi_t$ $\chi > \chi_t$